Mechanical Properties Characterization of Heat-Affected Zone Using the Small Punch Test

Use of the small punch test for the mechanical characterization of small areas such as the different zones that characterize the HAZ showed promise

BY C. RODRÍGUEZ, J. GARCÍA CABEZAS, E. CÁRDENAS, F. J. BELZUNCE, AND C. BETEGÓN

ABSTRACT

The small punch test (SPT) allows us to make mechanical characterizations of very small regions in any material as it uses very small test specimens ($10 \times 10 \times 0.5$ mm^3). The SPT can be used to characterize the heat-affected zones (HAZ) of welded joints, the mechanical properties of which are usually unknown, and which are the most problematic areas because of the possible existence of hard and brittle microstructures.

Since the SPT can be used to obtain mechanical properties (yield strength, ultimate strength, elongation, fracture energy, and toughness) of small regions, this test was used to evaluate how these properties change inside the HAZ of a welded joint made on a quenched and tempered steel. Several specimens were machined along the HAZ and the corresponding SPTs were performed at room temperature, using a hardness measurement of HV0.5 as a reference. In this case, the strength properties and hardness increase as we move away from the fusion boundary, but the elongation and fracture energy decrease.

Introduction

The mechanical behavior characterization of structural components, except in the case of hardness measurements, is always destructive since it requires direct extraction of large specimens for testing, machined from the real components to be evaluated.

For this reason, if we want to evaluate a component and introduce only minimum damage, it would be very convenient to use miniature tests for their mechanical characterization, making use of very small specimens (miniature samples) that could be extracted from the components during their normal service life, and which usually do not fulfill the requirements established in the corresponding standards. In the course of the last few years, different specimens with the same geometry but smaller than the standard ones were used for the evaluation of tensile, fatigue, fracture mechanics, impact properties, etc. Anyway, these results need to be reworked to derive the properties of the components, which are much larger than the tested samples (Refs. 1, 2).

These problems are especially relevant in the case of weld joints, where the existence of small heat-affected zones (HAZ) can produce serious problems during the design and manufacturing phases, although they can be solved or minimized using appropriate welding procedures and techniques. But in any case they always introduce some degree of uncertainty on the mechanical behavior of these regions under real service loads since, due to the small dimension of these HAZs (usually only some mm wide), it is not possible to characterize them using standard mechanical tests.

In the aforementioned situations, one of these miniature tests is the small punch test (SPT). Since the SPT uses small square specimens measuring 10×10 mm^2 with a thickness of 0.5 mm, it may be considered a quasi nondestructive test as the material removed is very low. In this work the use of the SPT was analyzed to obtain the tensile properties (yield stress, ultimate tensile strength, and elongation) of the HAZ produced during the course of a welding procedure performed on a quenched and tempered steel.

KEYWORDS

Heat-Affected Zone (HAZ)
Mechanical Properties
Small Punch Test (SPT)
Quenched and Tempered Steels

The Small Punch Test

The small punch test is a testing procedure that can be considered nearly nondestructive because of the small samples that are used (usually with a section of 10×10 mm and a thickness of 0.5 mm) (Refs. 3–6). Compared with other real nondestructive tests, such as X-ray diffraction, ultrasound, or magnetic techniques that are based on indirect measurements of the mechanical properties, the SPT allows us to directly obtain these properties.

In this test, the square specimen is firmly clamped between two circular dies and is strained until failure into a 4-mm-diameter cavity using a 2.5-mm-diameter hemispherical punch, as shown in Fig. 1. The tests were performed at a displacement rate of 0.2 mm/min.

The applied load and deflection of the specimen central point (DCP) measured with the help of a crack opening displacement (COD) type extensometer are recorded during the test. Figure 2 shows a typical load-DCP curve of ductile materials like those we used in this work. In this curve are marked different zones corresponding to the different states of deformation that the specimen will suffer.

Zones I and II correspond to states of bending deformation. Zone I corresponds to elastic bending and includes the linear portion of the curve, while Zone II corresponds to plastic bending. For specimens of standardized geometry and for the same testing machine, these curves are determined by the elastic-plastic material properties, i.e., the elastic modulus, yield stress σ_{ys}, and hardening coefficient of the material. From a certain moment onward, bending leads to a membrane regime, which predominates in most of the curve and corresponds to Zone III. This phase ends with fracture of the specimen. In the curve represented in Fig. 2, final fracture

C. RODRÍGUEZ, E. CÁRDENAS, F. J. BELZUNCE, and C. BETEGÓN are with Instituto Universitario de Tecnología Industrial de Asturias (IUTA), Universidad de Oviedo. J. GARCÍA CABEZAS is with General Dynamics Santa Bárbara Sistemas Oviedo, Asturias.

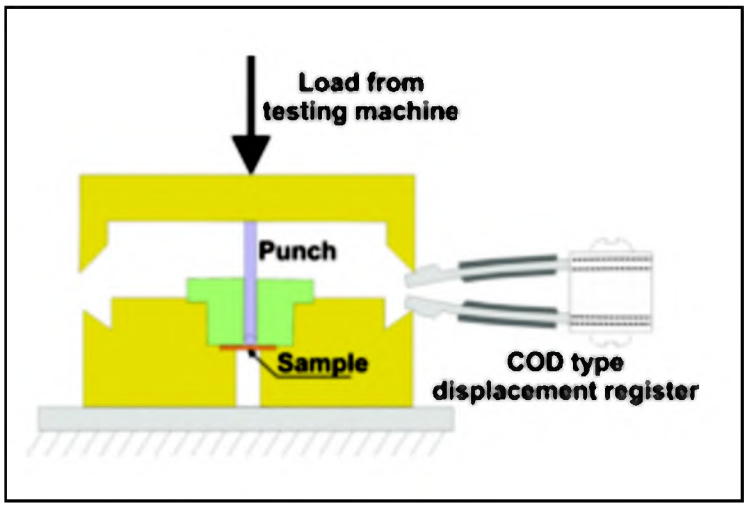

Fig. 1 — Schematic representation of the SPT equipment.

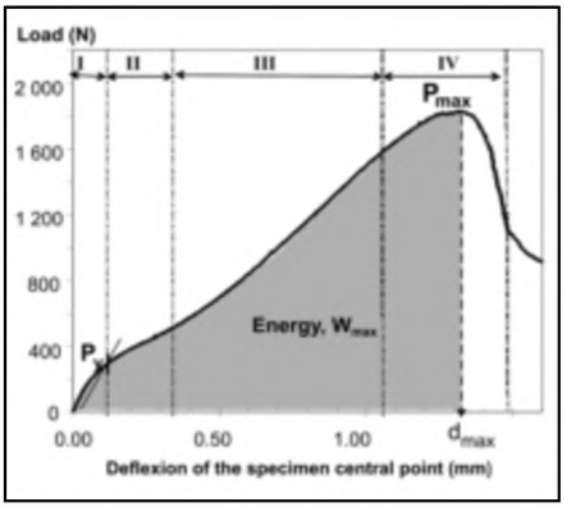

Fig. 2 — SPT load-deflection curve and identification of critical parameters.

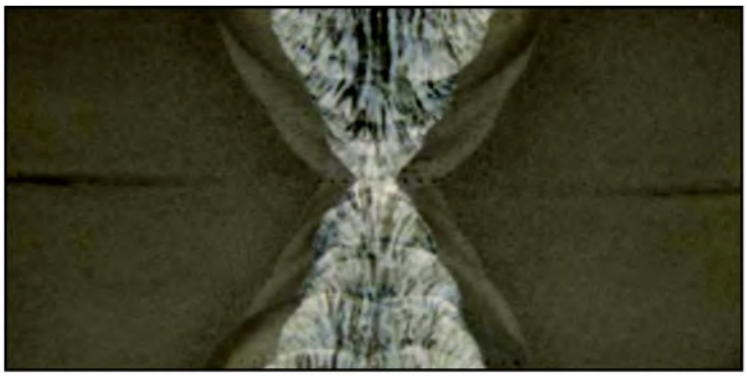

Fig. 3 — Macrograph of the welded joint.

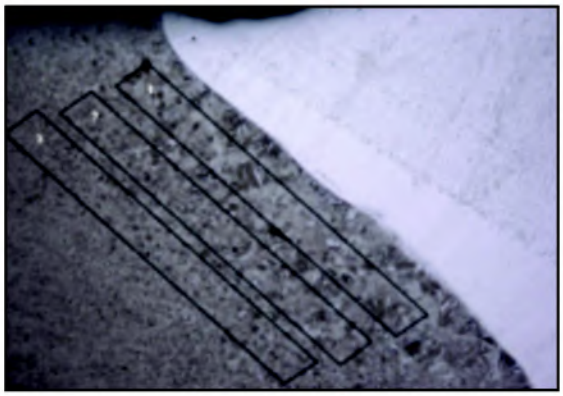

Fig. 4 — Microstructure of the different zones of the HAZ, which includes the situation of the extracted samples.

occurs as a result of the formation of a neck similar to that developed in tension tests of ductile materials and the subsequent formation of a crack in this location. The fracture of the specimen defines Zone IV, which includes the point of maximum load. In addition to the mechanical properties of the material, this point of maximum load depends on the coefficient of friction between the punch and the sample being tested, such that the higher this coefficient is, the greater is the load and the fracture location moved away from the center of the dome (Ref. 7).

This load-deflection curve is the only information collected in the small punch test and thus the only one at our disposal to ascertain the different material properties. Due to the complexity of the stress state that develops during the test, the work developed so far has focused on establishing empirical relationships between different mechanical properties and certain characteristic points of the curves, also marked on the curve in Fig. 2 (Refs. 8–11):

• $(P/d)_{ini}/t$, where $(P/d)_{ini}$ is the initial slope measured in the elastic region (Zone I) and t is the initial thickness of the specimen. This parameter is closely related with the tensile Young's modulus E.

• P_y/t^2, where P_y is the load where plastic strain starts, and it is obtained drawing a straight line parallel to the initial slope of the graph, but displaced $t/10$ — Fig. 2 (Ref. 12). This parameter is directly related to the material yield stress, σ_{ys}. The following expression is commonly used:

$$\sigma_{ys} = \alpha \cdot \frac{P_y}{t^2} \qquad (1)$$

where α is a material parameter.

• P_{max}/t^2, where P_{max} is the maximun load registered in the test. This parameter is directly related to the ultimate tensile strenght, σ_u by means of expressions like the following:

$$\sigma_u = \beta_1 \cdot \frac{P_{max}}{t^2} + \beta_2 \qquad (2)$$

where β_1 and β_2 are parameters related to the tested material and the friction coefficient between the punch and the sample.

• d_{max}/t is the deflection at the point of maximum load adimensionized by the thickness of the sample, and it is directly related to the tensile elongation e, by means of the following expression:

$$e(\%) = \gamma \cdot \frac{d_{max}}{t} \qquad (3)$$

where, again, γ is a characteristic material parameter.

• W_{max}/t^2 is now W_{max}, the energy absorbed at the point of maximum load (area under the SPT curve), which is related to the material toughness.

Material and Experimental Procedure

The material used in this study was the HAZ of a welded joint made using a 30CrMo5-2 plate with a thickness of 25 mm as base material and an austenitic stainless steel EN 1600 18 8 Mn B22 (ER 307-15 MOD) as filler metal. The chemical composition of both materials is shown in Table 1.

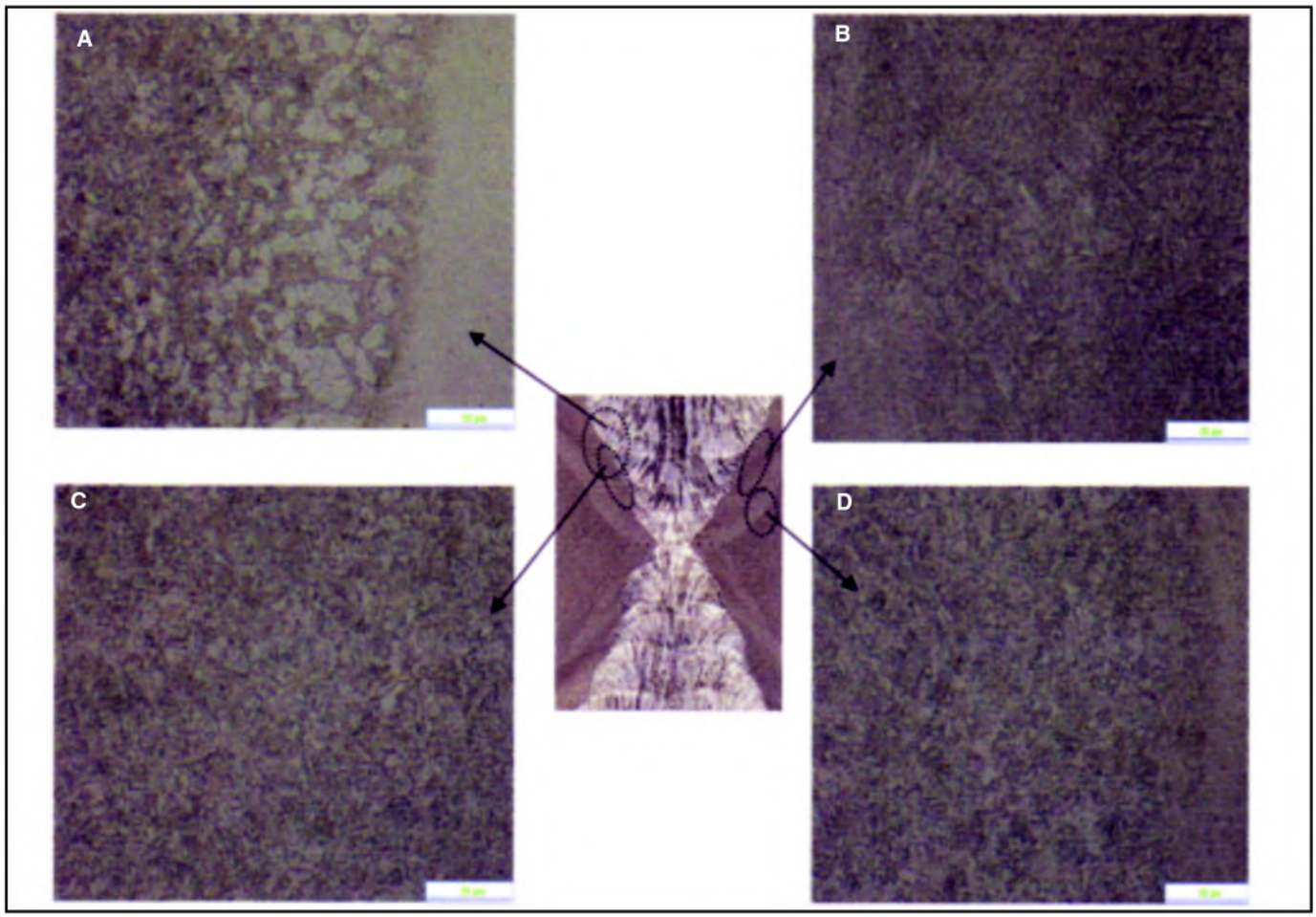

Fig. 5 — Microstructural evolution from the fusion boundary to the base metal. A — Fusion boundary; B — HAZ coarse grain; C — HAZ fine grain; D — HAZ intercritical.

Table 2 gives the conventional mechanical properties (tensile and hardness) of the base metal in the original state that corresponds to a quenched and tempered treatment (tempered at 500°–550°C), as recommended by the TL2350-000 standard (Ref. 13).

The coupons were butt joints that were double-beveled (X), multipass welded using a straight bead technique. A SMAW process with 4-mm-diameter electrodes was used.

Figure 3 is a macrograph of the welded joint, which shows a HAZ with a width of about 4.5 mm.

The microstructure of the joint was studied using a Nikon Eclipse ME 600 optical microscope. Hardness test profiles (Vickers hardness with a load of 0.5 kg) were performed at the root and also near the top and the bottom surfaces of the joint using a Future-Tec FM700 microhardness tester. Figure 4 shows the general microstructure of the joint, in which we can appreciate the fusion boundary and different zones of the HAZ.

Once the different zones of the HAZ were located, three rectangular samples parallel to the fusion boundary, with a thickness of 0.5 mm and different distances from the fusion boundary, were electrodischarge machined from the HAZ — Fig. 4. As can be see in Fig. 4, these samples were consecutively numbered from 1 to 3 as they separate from the fusion boundary and at least three 10 × 10 mm^2 SPT specimens were cut off for each one.

The SPT tests were carried out using an experimental device designed and manufactured at Instituto Universitario de Tecnología Industrial de Asturias (IUTA) (Ref. 12) mounted in a universal Instron testing machine having a load cell of 10 kN. The test fixture was manufactured using a quenched and tempered DIN 42CrMo4 steel (UNE 36051-91 (1) standard) with a final N6 grinding surface.

Table 1 — Chemical Compositions of Base and filler Metals (wt-%)

Material	C	Si	Mn	Cr	Mo	Ni	Al
BM[a]	0.27–0.33	0.1–0.4	0.5–0.8	1–1.5	0.1–0.3	—	<0.05
FM[b]	0.08	0.9	7	19.2	0	9	0.28

(a) Base metal chemistry is from TL2350-000 standard(Ref. 13).
(b) Filler metal chemistry is from 3.1B ISO supplier certificate (AWS A5.9-93 ER 307-15 mod No. 1.4370 EN 12072 G 18 8 Mn).

Table 2 — Minimum Mechanical Properties of Quenched and Tempered 30CrMo5-2 Steel (Ref. 13)

Material	σ_{ys}(MPa)	σ_u(MPa)	e(%)	HB10
BM	900	1000	15	290

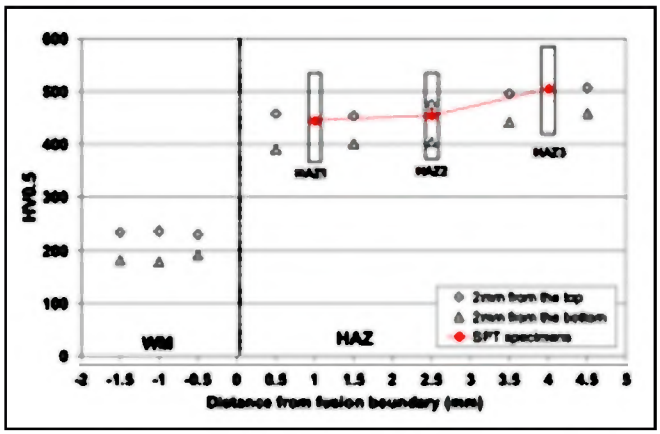

Fig. 6 — HV0.5 hardness profiles in different areas of the welded joint.

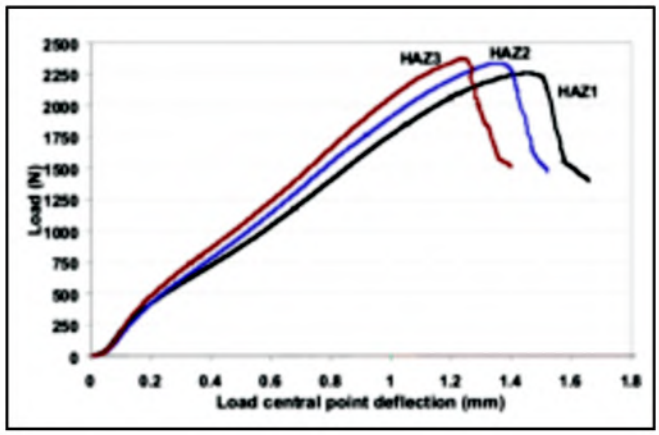

Fig. 7 — Representative SPT curves from the different HAZ zones.

The applied load vs. the deflection of the specimen's central point was registered in all these tests until the final failure of the specimens.

Results and Discussion

Microstructure and Hardness Profiles

As can be seen in Fig. 4, the HAZ shows a slight decarburation located next to the fusion boundary, which is due to the use of a filler metal with a very low carbon (austenitic stainless steel). Figure 5A–D give the microstructural evolution from the fusion boundary to the base metal of the welded joint. A general microstructure of tempered martensite was seen in both the HAZ and base material.

Figure 6 shows the HV0.5 hardness profiles measured at two positions located 2 mm from the top and bottom surfaces. Apart from the very low hardness of the filler metal (austenitic stainless steel), the hardness of the HAZ slightly increases as we move away from the fusion boundary, due to the tempering effect produced by the welding passes.

Figure 6 also represents the values obtained directly on the small punch tested specimens also using the HV0.5 hardness test. Similar to the anterior results, hardness measured on SPT specimens also increased away from the fusion boundary.

Small Punch Test Results

Table 3 collects the values of the characteristic parameters obtained in the SPTs once they were normalized, taking into account the thickness of the specimen. The average values and the standard deviations are also given in the same table.

Figure 7 shows three characteristic load-displacement curves representative of the three zones of the studied HAZ — Fig. 4. It is clearly seen that as it separates from the fusion boundary (from HAZ 1 to HAZ 3) the behavior of the material becomes more rigid, attaining higher loads and lower failure displacements.

Although there was some dispersion, as is normal in this type of test, consistent and repetitive results were nevertheless obtained, which justify that the experimental technique used is accurate enough. On the other hand, the P_y/t^2 and the P_{max}/t^2 parameters (proportional to the yield stress and to the ultimate tensile strength, respectively) increase, whereas the d_{max}/t and W_{max}/t^2 parameters (proportional respectively to the tensile elongation and to the fracture energy) decrease as we get away from the fusion boundary. These results fully agree with the hardness and microhardness results already represented in Fig. 6.

From these SPT characteristic parameters, it is possible to get the tensile mechanical properties (σ_{ys}, σ_u, and e) of the

Table 3 — Normalized Characteristic SPT Parameters (Mean Values and Standard Deviation)

Specimen Number	Thickness, t (mm)	$(P/d)_{ini}/t$ (MPa)	$P_y(t/10)/t^2$ (MPa)	P_{max}/t^2 (MPa)	d_{max}/t	W_{max}/t^2 (kJ/m²)
HAZ1P1	0.469	7221.75	2000.35	10263.18	3.0944	4
HAZ1P2	0.467	7793.36	2292.64	10756.21	3.0148	4.31
HAZ1P3	0.462	5987.01	2000.52	10234.38	3.2693	4.34
HAZ1	**Mean val.**	**7000.71**	**2097.84**	**10417.92**	**3.13**	**4.21**
	St. Dev.	**923.24**	**168.7**	**293.32**	**0.1302**	**0.188**
HAZ2P1	0.473	7097.25	2503.03	10714.5	2.93478	4.16
HAZ2P2	0.474	7445.99	2492.48	10189.8	2.98114	3.8
HAZ2P3	0.468	6854.7	2387.87	10685.7	2.90653	3.978
HAZ2	**Mean val.**	**7132.65**	**2461.12**	**10530.01**	**2.94**	**3.98**
	St. Dev.	**297.23**	**63.66**	**294.97**	**0.0377**	**0.180**
HAZ3P1	0.468	8199.57	2636.7	10754	2.72454	3.706
HAZ3P2	0.4802	7887.76	2680.06	10577.1	2.64742	3.638
HAZ3P3	0.477	7662.47	2685.37	10448.7	2.61141	3.515
HAZ3	**Mean val.**	**7916.6**	**2667.38**	**10593.3**	**2.66**	**3.62**
	St. Dev.	**269.71**	**26.70**	**153.29**	**0.0578**	**0.096**

different HAZs (HAZ 1, HAZ 2, and HAZ 3) by just applying Equations 1, 2, and 3 using the appropriate coefficients.

In the case of coefficient α, most of the authors indicate a value around 0.36 for ferritic steels and around 0.41 for martensitic steels (Refs. 14–16). As we have characterized a quench and tempered martensitic steel, an α value of 0.38 was employed (Ref. 17). Table 4 shows the yield strength calculated in this way.

In the same table, tensile strength and elongation were also obtained after applying Equations 2 and 3, respectively, using the β_1, β_2, and γ parameters proposed by Ruan et al. (Ref. 11), and Fleury and Ha (Ref. 8) for steels similar to the steel used in this study.

The results presented in Table 4 show a clear increase in the yield strength as we get off the fusion boundary, while the increase in tensile strength and the decrease in elongation are already less significant. These values are also in the same range, although a little bit higher, than the same base metal properties (Table 2) and can be easily justified due to the tempering effect produced on the HAZ by the welding passes.

Table 4 — Mechanical Properties of the Different Areas of the HAZ Obtained from Equations 1–3

Material	$\sigma_{ys} = \alpha \cdot \frac{P_y}{t^2}(MPa)$	$\sigma_u(MPa) = \beta_1 \cdot \frac{P_{max}}{t^2}\left(\frac{kN}{mm^2}\right) + \beta_2$	$e(\%) = \gamma \cdot \frac{d_{max}}{t}(\%)$
	$\alpha = 0.38$	$\beta_1 = 77,\ \beta_2 = 218$	$\gamma = 7$
HAZ1	797.2±64	1020±23	21.9±0.9
HAZ2	935±25	1029±23	20.6±0.3
HAZ3	1014±20	1034±12	18.6±0.4

Conclusions

The possibility of using the small punch test (SPT) for the mechanical characterization of small areas such as the different zones that characterize the HAZ of a welded joint is very promising as was shown in the case of a quenched and tempered steel.

Three characteristic zones from the fusion boundary to the base metal of a shielded metal arc welded joint with a HAZ roughly 4.5 mm wide were differentiated and checked by means of hardness and small punch tests. Away from the fusion boundary, hardness increases, as do the SPT strength parameters, while the ductility and toughness SPT parameters decrease. Afterward, using expressions previously validated, approximated values of the yield strength, tensile strength, and elongation were also calculated.

This work confirms the promising future of the SPT for the mechanical characterization by means of miniature samples of small zones, such as the HAZ of welded joints.

Acknowledgments

The authors gratefully acknowledge funding from the Spanish Science and Education Ministry provided via project DGICYT (MAT-2004-06992-C02-01).

References

1. Lucon, E. 2001. Material damage evaluation and residual life assessment of primary power plant components using specimens of nonstandard dimensions. *Mater. Scie. Tech.* 17: 777-s to 785-s.

2. Lucas, G. E., et al. 2002. Recent progress in small specimen test technology. *J. Nucl. Mater.* 307–311: 1600-s to 1608-s.

3. Manahan, M. P., et al. 1981. The development of a miniaturized disk bend test for determination of postirradiation mechanical properties. *J. Nucl. Mater.* 103–104: 1454-s to 1550-s.

4. Mao, X. Y., and Takahashi, H. 1987. Development of a further miniaturized specimen of 3 mm diameter for TEM disk small punch tests. *J. Nucl. Mater.* 150: 42-s to 52-s.

5. Parker, et al. 1995. Deformation and fracture processes in miniature disc tests of CrMoV rotor steel. *Proc. 3rd. Int. Charles Parsons Turbine Conf.*, 2, 418–428.

6. Bicego, et al. 1995. Integrated technologies for life assessment of primary power plant components. *Proc. Int. Symp. on Materials Aging and Components Life Extension* 1: 295–305.

7. Hosford, W. F., and Caddel, R. M. 1983. *Metal Forming: Mechanics and Metallurgy.* Prentice-Hall Inc.

8. Fleury, E., and Ha, J. S. 1998. Small punch tests to estimate the mechanical properties of steels for steam power plant. *Int. J. Press. Vessels and Piping* 75: 699-s to 706-s.

9. Vorlicek, et al. 1995. Evaluation of a miniaturized disc test for establishing the mechanical properties of low-alloy steels. *J. Mater. Scie.* 30: 2936-s to 2943-s.

10. Foulds, J., and Viswanathan, R. 2001. Determination of the toughness of in-service steam turbine disks using small punch testing. *J. Mater. Eng. Perform.* 10(5): 614-s to 619-s.

11. Ruan, Y., Spätig, P., and Victoria, M. 2002. Assessment of mechanical properties of the martensitic steel EUROFER97 by means of punch tests. *J. Nucl. Mater.* 307–311: 236-s to 239-s.

12. Autillo, J., Contreras, M. A., Betegón, C., Rodríguez, C., and Belzunce, F. J. 2006. Utilización del ensayo miniatura de punzonamiento en la caracterización mecánica de aceros. *Anales de Mecánica de la Fractura.* 23: 77-s to 83-s.

13. TL2350-000 standard (1997) Germany, "Restricted."

14. Campitelli, E., Spatig, P., Bonade, R., Hoffelner, W., and Victoria, M. 2004. Assessment of the constitutive properties from small ball punch test: Experimental and modeling. *J. of Nuclear. Materials* 335: 366-s to 378-s.

15. Finarelli, D., Roeding, M., and Carsughi, F. 2004. Small punch tests on austenitic and martensitic steels irradiated in a spallation environment with 530 MeV protons. *J. of Nuclear Materials* 328: 146-s to 150-s.

16. Contreras, M. A., Rodríguez, C., Belzunce, F. J., and Betegón, C. 2008. Use of small punch test to determine the ductile-to-brittle transition temperature of structural steels. *Fatigue Fract Engng Mater Struc.* 31: 727-s to 737-s.

17. Rodríguez, C., Belzunce, F. J., Betegón, C., and Contreras, M. A. 2008. Uso del EMP para la caracterización mecánica de zonas afectadas térmicamente en uniones soldadas. *Soldadura y Tecnologías de Unión* 109: 16-s to 21-s.